

# Enhancement of Small Signal Stability of Wind Farms by Using STATCOM and HVDC Link

Omar AL-Masari, Musa AL-Masari

**Abstract**— *Small signal instability problems in wind farms often lead to power system blackouts. This paper reports a comprehensive study of small signal stability in three different types of wind generator when coupling to a power system: doubly-fed induction generators (DFIG), squirrel cage induction generators (SCIG) and permanent magnet synchronous generators (PMSG). Time-domain analysis and Eigenvalue analysis were used to identify small signal instability problems in wind farm power systems. A static synchronous compensator (STATCOM) and power system stabilizer (PSS) was modelled and applied to the power system to enhance small signal stability. In addition, the performance of high voltage direct current (HVDC) and high-voltage alternating current (HVAC) links was examined in connecting the wind farm to the grid. The results show improvement in small signal stability by using HVDC rather than HVAC. The IEEE 14 Bus test system and all simulation models were implemented using the DIgSILENT PowerFactory software tool.*

**Index Terms**— *Wind Turbine Generators, Small Signal Stability, Oscillatory Stability, Eigenvalue analysis, SCIG, PMSG, DFIG, STATCOM, PSS, HVDC, HVAC, IEEE 14 Bus test system, DIgSILENT PowerFactory.*

## I. INTRODUCTION

As many countries turn to renewable energy resources to ensure conservation of the environment and security of future energy supply, wind energy has become one of the most reliable sources of free energy worldwide. The advantages of wind energy as a response to global warming include reduced burning of fossil fuels, no CO<sub>2</sub> emissions and reduced installation costs of wind turbine generators (WTGs), leading to increased demand for this form of power [1]. At present, around 20% of the renewable energy supply worldwide comes from wind energy, and this figure is expected to reach 25% by 2035 [2, 3]. This growing demand for energy from wind presents a challenge for the operators and planners of power systems, who must ensure safe and reliable operation, and implementation of large-scale wind farms is expected to be high for decades to come. As the demand for wind-based power generation increases, it becomes essential to more fully understand wind power system stability [4].

When interconnection between power systems was first introduced in 1960, instability problems included voltage stability, frequency stability and small signal stability [5]. Although interconnection in power systems has since improved, there is a growing concern about the impact of interconnections on small signal stability, as power system blackouts can in many cases be attributed to small signal

instability problems.

In essence, small signal stability is the ability of a power system to retain equilibrium or synchronism when subjected to small disturbances [6]. In the absence of adequate damping, these disturbances may lead to system blackout, but in most cases these disturbances simply dissipate within a short time and the system can return to its stable operating point. This problem is usually related to a lack of sufficient damping of system oscillations, sudden changes in load or short circuit events [7]. To improve small signal stability, a power system stabilizer (PSS) was introduced to synchronous generators to add more damping to the system and so enhance small signal stability [5]. This methodology was an effective solution for systems involving a single machine connected to infinite bus. However, in multi-machine power systems and when connecting more than one PSS in the system, these PSSs can cause small signal instability and produce negative damping oscillation [8]. One study of the main causes of oscillatory instability found that poor design of PSSs was one cause of instability problems in power systems [9]. In another study [10], power system stabilizers (PSS) and HVDC links were introduced to add more damping in an attempt to reduce instability issues. It is reported that the presence of HVDC systems can improve the stability of a network by add more damping. However, the effect of HVDC systems on small signal stability for all three types of wind generators has not to date been investigated. To that end, the present study examined the capacity of STATCOM, PSS and HVDC to enhance small signal stability under different modes of operation.

The main goal of this research paper is to investigate and analyse wind farm small signal stability, and then to apply controllers to the enhancement of instability. The paper is structured as follows. Section II describes in detail the methodology used for the small signal stability study. Section III presents the eigenvalue classification. Section IV provides modelling of the wind power system, the STATCOM model, the HVDC link and the IEEE 14 Bus test system. Section V describes the simulation and results, followed by conclusions in Section VI.

## II. METHODOLOGY

As in previous studies, eigenvalue analysis and time-domain simulations are used here to analyse small signal stability [8, 11]. This kind of analysis can be done by linearising the system around an equilibrium point that represents the steady-state operating condition. System equations can be formulated by starting from nonlinear ordinary differential equations that can be linearised at the operating point [6].

**Manuscript Received on February 2015.**

**Omar Almasari**, School of Information Technology and Electrical Engineering, University of Queensland, Brisbane, Australia.

**Musa Almasari**, Electrical Engineering, University of Windsor, Windsor, Ontario.

$$\dot{x} = f(x, u, t), \quad (1)$$

where x is the state variable, u is the input variable, and t is the time.

$$\dot{x} = f(x, u) \quad (2)$$

The output variables can be

$$y = g(x, u). \quad (3)$$

Linearisation

$$\dot{x} = f(x_0, u_0) = 0 \quad (4)$$

$$x = x_0 + \Delta x; \quad (5)$$

$$u = u_0 + \Delta u \quad (6)$$

$\Delta$ =small deviation

Substitute x and y with a small deviation

$$\dot{x} = \dot{x}_0 + \dot{\Delta x} \quad (7)$$

$$= f[(x_0 + \Delta x), (u_0 + \Delta u)] \quad (8)$$

A nonlinear function can be expressed as a Taylor Series

$$x_0 + \Delta x = f_1[(x_0 + \Delta x), (u_0 + \Delta u)] \quad (9)$$

$$= f_1(x_0, u_0) + \frac{\partial f_1}{\partial x_1} \Delta x_1 + \frac{\partial f_1}{\partial x_2} \Delta x_2 + \dots + \frac{\partial f_1}{\partial x_n} \Delta x_n + \frac{\partial f_1}{\partial u_1} \Delta u_1 + \frac{\partial f_1}{\partial u_2} \Delta u_2 + \dots + \frac{\partial f_1}{\partial u_r} \Delta u_r. \quad (10)$$

Linearisation

$$\begin{aligned} \dot{x}_{01} &= f_1(x_0, u_0) \\ \Delta \dot{x}_{01} &= \frac{\partial f_1}{\partial x_1} \Delta x_1 + \frac{\partial f_1}{\partial x_2} \Delta x_2 + \dots + \frac{\partial f_1}{\partial x_n} \Delta x_n \\ &+ \frac{\partial f_1}{\partial u_1} \Delta u_1 + \frac{\partial f_1}{\partial u_2} \Delta u_2 + \dots + \frac{\partial f_1}{\partial u_r} \Delta u_r \end{aligned} \quad (11)$$

or

$$\Delta \dot{x} = A \Delta x + B \Delta u \text{ this from linearise } \dot{x} = f(x, u)$$

$$\Delta \dot{y} = C \Delta x + D \Delta u \text{ this from linearise } \dot{y} = g(x, u)$$

A, B, C, and D are matrices with partial derivative terms, where A is the state matrix, B is the control matrix, C is the output matrix, and D is the feed forward matrix.

$$\det(SI - A) = 0 \quad (12)$$

We can rewrite the previous equation as

$$\det(\lambda I - A) = 0 \quad (13)$$

The eigenvalues of state matrix A are given by the values of the scalar parameter

$$\lambda = \alpha \pm j\beta, \quad (14)$$

where  $\alpha$  is the real part of the eigenvalues and  $\beta$  is the complex part of the eigenvalues.

$$\text{Damping ratio } \zeta = \frac{-\alpha}{\sqrt{\alpha^2 + \beta^2}} \quad (15)$$

$$\text{Frequency } f = \frac{\beta}{2\pi} \quad (16)$$

The damping ratio can determine the rate of decay of the amplitude of the oscillation stability. Frequency can determine the oscillatory stability modes.

### III. PROPERTIES OF EIGENVALUES

In order to understand system oscillation modes, frequency and damping ratios must be calculated. These provide information about the system instability mode. Three main properties of system instability can be described in terms of eigenvalues [5], as follows:

(1) If all the eigenvalues of the system have negative real parts after linearising, the system is asymptotically stable.

(2) If the system has at least one eigenvalue with positive real parts, the system is unstable.

(3) If all the eigenvalues of the system have negative real parts other than one complex pair having purely imaginary values, the system exhibits oscillatory motion.

## IV. WIND POWER SYSTEM

### A. The Aerodynamics Model

The maximum mechanical power output of a wind turbine is presented by the following equation:

$$P_m = \frac{1}{2} \rho A C_p(\lambda, \beta) v_w^3, \quad (17)$$

where  $P_m$  is the mechanical power [W], ( $\rho = 1.225 \text{ [kg/m}^3\text{]}$ )  $\rho$  is the air density,  $A$  is the areas swept by the wind turbine bald, ( $A = \pi R^2 \text{ (m}^2\text{)}$ ),  $C_p(\lambda, \beta)$  is the power coefficient of wind turbine,  $v_w$  is the wind speed [m/s],  $\beta$  is the pitch,  $\lambda$  is the tip speed ratio, and  $v_t/v_w$  is the ratio between the blade tip speed  $v_t$  and the wind speed.

The tip speed ratio ( $\lambda$ ) is related to the power coefficient defined as

$$\lambda = \frac{R \omega_r}{v_w}, \quad (18)$$

where R is the radius of rotor bald in meters and  $\omega_r$  is the rotor speed in pu.

The power coefficient can be calculated by using

$$C_p(\lambda, \beta) = 0.73 \left( \frac{151}{\lambda} - 0.58\beta - 0.002\beta^{1.4} - 13.2 \right) e^{\left( \frac{-19.4}{\lambda} \right)} \quad (19)$$

$$\lambda = \left( \frac{1}{\lambda - 0.112\beta - (\beta^2 - 1)} \right).$$

### B. Pitch Angle Controller

The pitch angle controller is used to adjust wind turbine blade pitch when the wind speed is high. Pitch angle must be kept constant at low wind speeds between zero and one. Figure 1 demonstrates the relation between power coefficient ( $C_p$ ) and tip-speed ratio ( $\lambda$ ); for a higher power coefficient ( $C_p$ ) corresponding to a lower pitch angle value ( $\beta=0$ ), maximum mechanical power is achieved for a lower wind speed.

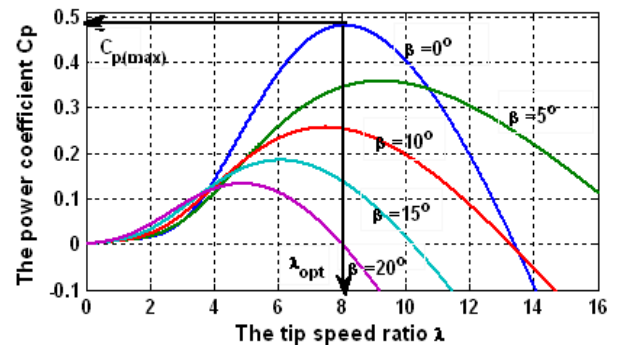


Fig 1: Power coefficient virus tip-speed [12].

### C. Wind Turbine Generators

Three different types of wind generator—squirrel cage induction generators (SCIG), permanent magnet synchronous generators (PMSG), and doubly-fed induction generators (DFIG)—are commonly used in wind energy production.

#### • Fixed speed wind turbine

The squirrel cage induction generator (SCIG) is commonly known as a fixed or constant speed wind generator because of the limitations on operating speeds. The SCIG is connected to the power system network by means of a step-up transformer (see Figure 2). A capacitor bank and soft starter are connected to manage and support the system with reactive power [13].

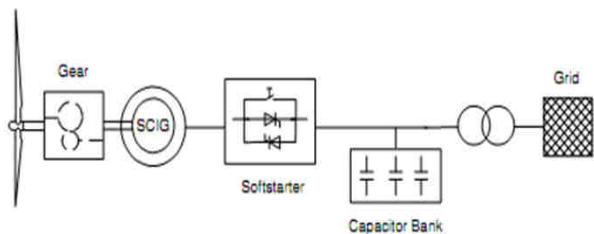


Fig 2: Squirrel cage induction generator wind system [14]

The main advantages of constant speed wind turbines are their simple construction and lower cost. However, there are some drawbacks, such as limitation in speed and control, low efficiency and more reactive power demand. These difficulties make this kind of system a poor choice for long-term investment [15].

• **Doubly-fed induction generator systems (DFIG)**

The doubly-fed induction generator (DFIG) is currently the most widely recognized device on the wind turbine market. A partial scale converter connects the rotor side of the DFIG to the grid (see Figure 3), enabling the range of operating speeds to be controlled electronically. This allows the DFIG to perform within a typical speed range of synchronous speed  $\pm 30\%$ , especially when the voltage source converter is adjusted to 20–30% of total turbine power [16].

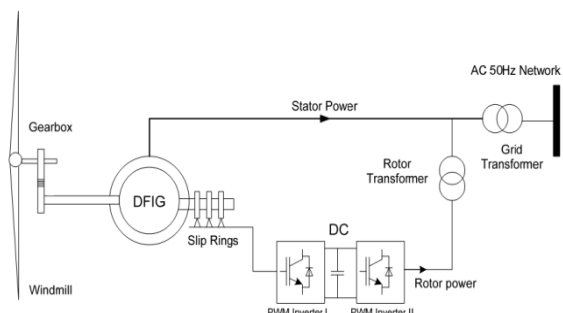


Fig 3: DFIG model [16]

• **Permanent magnet synchronous generator (PMSG)**

The permanent magnet synchronous generator (PMSG) is a synchronous generator which is connected to a full-scale frequency converter, and the generator is excited by placing a permanent magnet in the rotor (see Figure 4). The full back-to-back converter provides unlimited range speed control for connected generators [16].

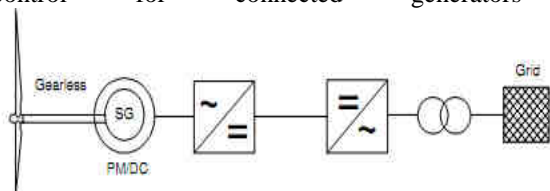


Fig 4: Permanent Magnet Synchronous Generator (PMSG) [18]

**D. High voltage DC link (HVDC).**

The main purpose of using a HVDC link is to connect two or more systems. HVDC transmission is the only means of connecting offshore wind farms, especially when high power is required over a long distance. The basic type of HVDC or DC link is monopolar (see Figure 5). This model can be considered as a DC link because it uses a distribution system [9].

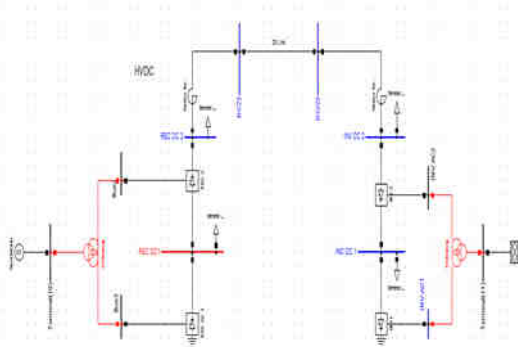


Fig 5: High voltage direct current (HVDC) link

HVDC links are found in many offshore wind farms [5, 9], for a number of reasons:

- To keep the rated power of the converter as high as possible for the given current and voltage ratings
- To minimize voltage drops at the AC connection point as loading increases
- To minimize the cost of the reactive power supply to the converters

**E. Power system stabilizers (PSS)**

Power system stabilizers (PSS) have been widely used since the introduction of interconnection between systems and the ensuing problem of oscillation instability. The main purpose of PSS in power systems is to damp electro-mechanical modes occurring when two or more systems are connected together. However, the location and tuning of PSS are major factors in adding more damping to the system. Using PSS with excitation systems is more effective in oscillatory instability [15] Figure 6 details the main controls of PSS.

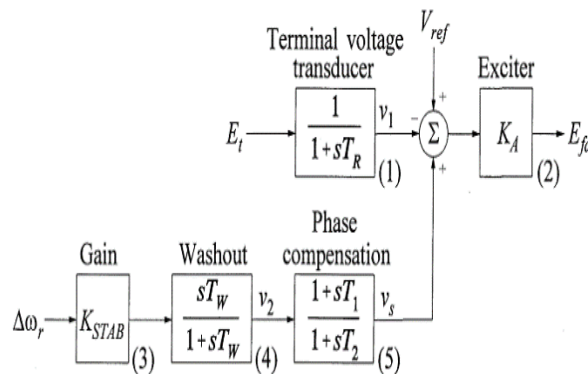


Fig 6: Power system stabilizer [5]

**F. Modelling of STATCOM**

The static synchronous compensator (STATCOM) is a voltage source converter (VSC) device. The voltage source is created from a DC capacitor that supplies STATCOM in order to increase active power support. [17].

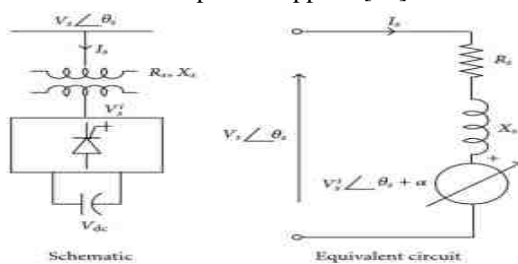


Fig 7: STATCOM model

V. RESULTS AND DISCUSSION

The IEEE 14 Bus test system was modelled with a rated voltage of 13.8 KV at 50 Hz and a total load of 259 MW and 81.3 MVar. More details about the system have been published elsewhere [18].

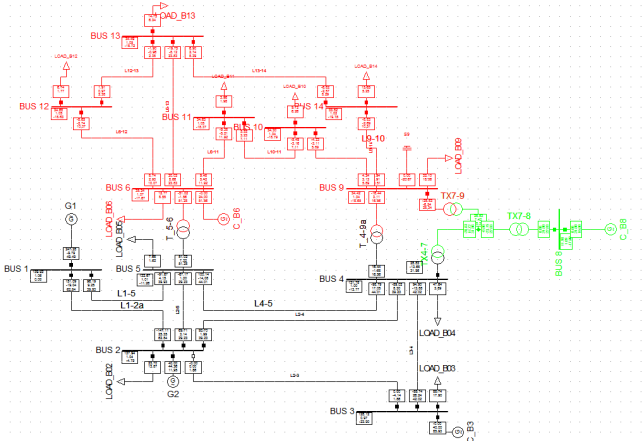


Fig 8: IEEE 14 Bus system

A. Analysis and Comparison of Eigenvalues of (SCIG), DFIG and PMSG Systems

Table 1 shows the damping ratio and frequency for SCIG, DFIG and PMSG wind turbines. From Table 1, it can be seen that SCIG has a global mode with frequency 0.6333244 HZ and damping ratio 0.6647432%. Local mode was found in the results for DFIG, which connects to the electric grid system with eigenvalue  $-0.99535 \pm 13.5918j$  and damping ratio 0.9953%. With a frequency of 7.536667 HZ, PMSG has good values, meaning that no oscillatory mode was found.

Table 1: Complex Eigenvalues of SCIG, DFIG and PMSG wind turbines

	Name	Eigenvalue	Frequency	Damping Ratio
		$\Lambda$	Hz	%
SCIG	Mode 1	$-0.66474 \pm 3.979295j$	0.633324	0.664743
DFIG	Mode 2	$-0.99535 \pm 13.5918j$	2.163202	0.995348
PMSG	Mode 3	$-4.528533 \pm 47.35428j$	7.536667	4.528533

Figure 9 shows all eigenvalues located in the left-half plane for all connected generators, indicating that all systems are stable. The location of a pair of complex eigenvalues for PMSG is better than both SCIG and DFIG which it's far from zero. It follows that PMSG can provide system stability by adding damping.

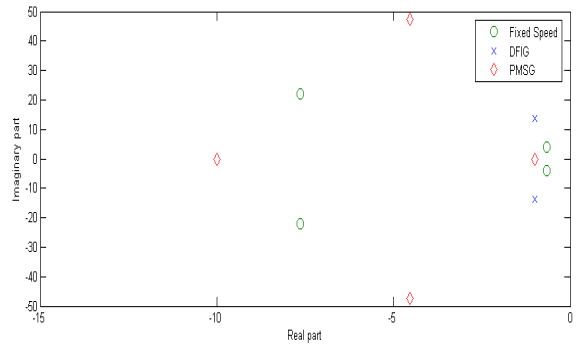


Fig 9: Comparison of the eigenvalues of fixed-speed (SCIG), DFIG and PMSG wind turbines

A time-domain analysis was conducted to compare the results for the three types of wind generators. In this simulation, a three-phase fault was applied near the grid side to assess the overall response and stability of the generators.

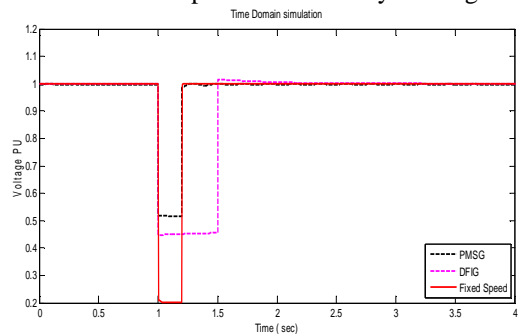


Fig 10: Comparison of time-domain simulations for PMSG, DFIG, and fixed-speed (SCIG) wind turbines

The results obtained from the time-domain analysis show that both DFIG and PMSG were able to recover from the fault within a few seconds while the fixed-speed (SCIG) turbine continues to dip when the same three-phase fault is applied (see Figure 10). This simulation shows that PMSG is an attractive choice for a wind energy system.

B. Analysis of an IEEE 14 Bus test system with PSS and STATCOM

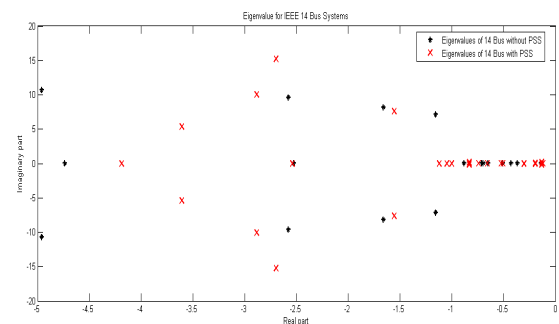


Fig 11: Comparison between Eigenvalues of IEEE 14 Bus with and without PSS

As can clearly be seen from Figure 11, the eigenvalues indicate that PSS adds more damping to the test system as compared to the system without PSS.

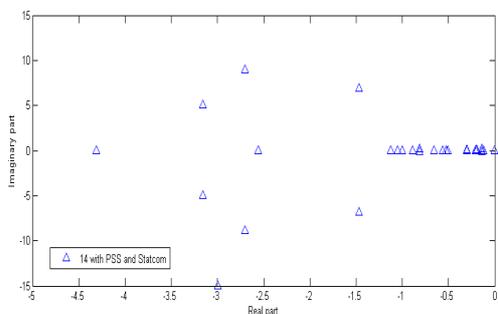


Fig 12: Comparison between eigenvalues of IEEE 14 Bus system with PSS and STATCOM

The graph above shows the simulation results for PSS and STATCOM. The results show that both PSS and STATCOM added more damping to the system and all eigenvalues improved, moving from 1.1 HZ to 1.5 HZ to local mode.

C. Analysis of SCIG wind farm connected to an IEEE 14 Bus test system via HVDC and HVAC

This simulation studied the effect of HVDC on wind farm small signal stability. The SCIG wind farm consisted of 25 machines with a capacity of 2 MW each, yielding a total capacity of 50 MW. The wind farm has the same specification as for the SCIG wind turbines discussed in the previous section. The wind farm was connected to the IEEE 14 Bus system via bus.

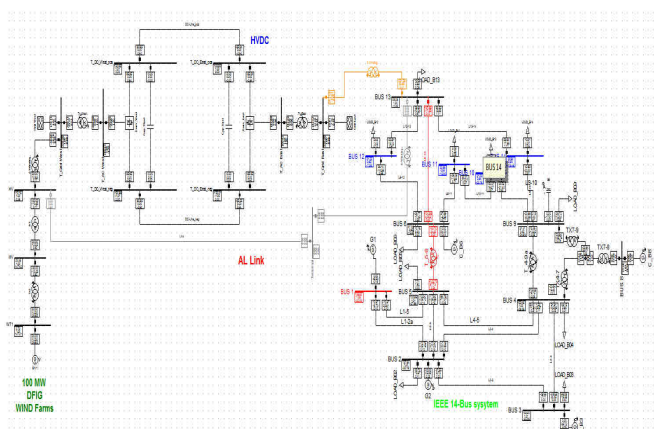


Fig 12: Location of wind farm connection to IEEE 14 Bus System via HVAC and HVDC links

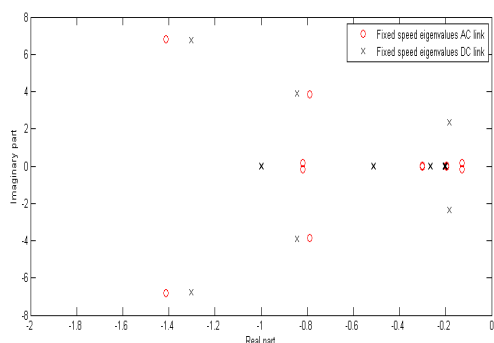


Fig 14: Comparison between eigenvalues of fixed speed wind farm connected to IEEE 14 Bus system via HVAC and HVDC links

Based on the eigenvalue graph in Figure 14, the system is stable as all eigenvalues have negative real parts. However,

the eigenvalues are located between -0.7 and -1, which means that oscillatory stability modes were introduced to the system when the large-scale wind farm was connected. Results obtained from connection to the fixed-speed wind farm via HVDC link show slightly improved damping with some critical damped modes, as seen in Figure 14.

Table 2: Selected eigenvalues of fixed-speed wind farm connected via HVAC link and HVDC link

	Name	Eigenvalue	Frequency	Damping Ratio
		$\Lambda$	Hz	%
SCIG (HVAC)	Mode 1	$-0.1279699 \pm 0.1585839 j$	0.0252394	62.7989
SCIG (HVDC)	Mode 1	$-0.184483 \pm 2.352037 j$	0.3743383	7.81952
SCIG (HVAC)	Mode 2	$-0.7885651 \pm 3.87381 j$	0.616536	19.9472
SCIG (HVDC)	Mode 2	$-0.8452583 \pm 2.352037 j$	0.6196149	19.9472
SCIG (HVAC)	Mode 3	$-1.411752 \pm 6.826279 j$	1.086436	20.25256
SCIG (HVDC)	Mode 3	$-1.302217 \pm 6.773321 j$	1.078007	18.8799

Table 2 shows that there are three oscillatory modes, mainly affecting local plant (1-2 HZ), inter-area (0.1-1 HZ) and some controls below 0.1 HZ. These results indicate some improvement in eigenvalue location in some critical damping modes, confirming that a HVDC link can enhance small signal stability. A time-domain simulation of the fixed-speed wind farm was therefore conducted.

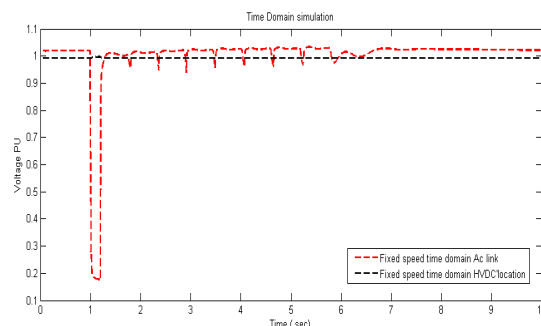
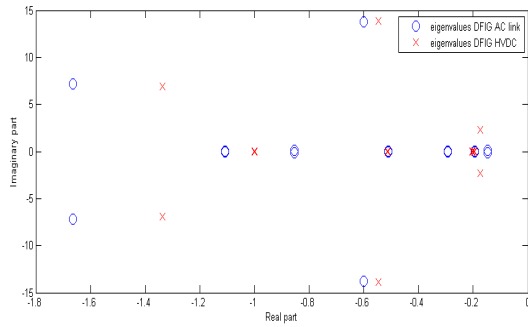


Fig 15: Comparison of SCIG wind farm for HVAC and HVDC links

Figure 15 demonstrates recovery time of the fixed-speed wind farm when three phase faults are applied at bus 13. When connected via HVAC, the wind farm took 6 seconds to recover after the fault was clear because of a lack of reactive power support in the system. However, with the HVDC link, the fixed-speed wind farm was unaffected by the three phase fault, which was blocked from reaching the wind farm. This confirms that the HVDC link has a significant impact on stability problems in wind power systems.

D. Analysis of a DFIG wind farm connected to an IEEE 14 Bus test system through a HVDC link

The DFIG wind farm consisted of 50 machines with a capacity of 2 MW, providing a total capacity of 100 MW. The wind farm was connected to the IEEE 14 Bus system via bus 13 (see Figure 13).



**Fig 16: Comparison between eigenvalues of DFIG wind farm connected to IEEE 14 Bus system via HVAC and HVDC links**

The eigenvalues based on the simulation result in Figure 16 show that DFIG stability is better with a HVDC link than with a HVAC link. The system is stable because all pair complex eigenvalues are in the left-half plane for both links. To confirm these results, a three phase fault was applied to connection bus 13. Figure 17 shows the DFIG wind farm's voltage recovery time.

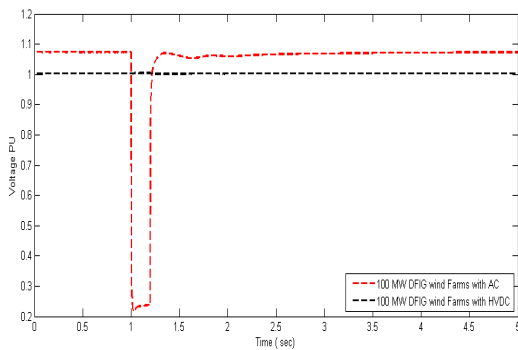


**Fig 17: Comparison of DFIG wind farm with HVAC and HVDC links**

The above graph shows the recovery time for the DFIG wind farm. When connected through a HVAC link, the system stabilised after the fault was cleared, and voltage stability and fault clearing time are within the acceptable range required by IEEE. However, the time-domain simulation shows that the DFIG wind farm with HVDC link was unaffected by the three phase fault, which was blocked.

### E. Analysis of a PMSG wind farm connected to an IEEE 14 Bus test system via HVDC and HVAC

The PMSG wind farm consisted of 50 machines with a capacity of 2 MW, providing a total capacity of 100 MW. The wind farm was connected to IEEE 14 Bus system via bus 13.

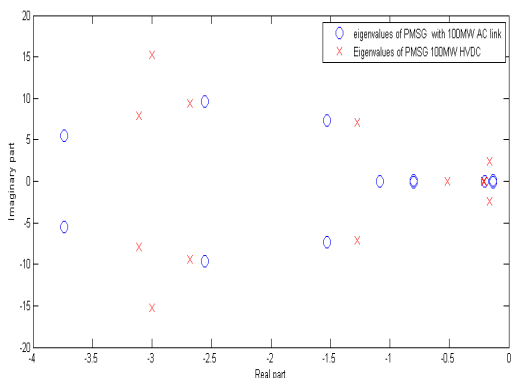


**Fig 18: Comparison between Eigenvalues of PMSG wind farm connect to IEEE 14 Bus system via HVAC and HVDC links**

Some small complex eigenvalues close to zero in Figure 18 can be ignored. The eigenvalue results for PMSG with HVDC link show improved damping of small signal stability. All complex pair of eigenvalues of the PMSG wind farm are in the left-half plane, indicating that this system is stable.

Time-domain analysis is recommended because of the introduction of some modes less than 0.01 HZ or at 0.001 HZ. A three phase fault was applied to the system at the connection point.

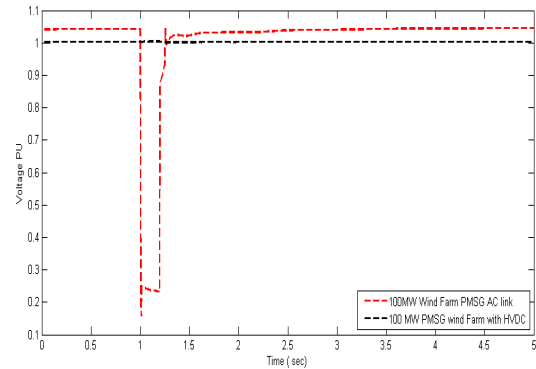


**Fig 19: Comparison of PMSG wind farm with HVAC and HVDC links**

Figure 19 shows the PMSG wind farm with HVAC and HVDC links. It is interesting that the PMSG wind farm showed the best clearing time. The time-domain result shows that recovery time for the PMSG wind farm when connected through a HVAC link is stable after clearing the fault.

## VI. CONCLUSION

Small signal analysis approaches such as eigenvalue and time-domain analyses can identify system problems and provide additional information about wind turbine models. Controllers such as STATCOM, PSS and HVDC links were applied to wind farms to address small signal instability problems. Based on the simulation results, the conclusions can be summarized as follows.

- Analysis of IEEE-14 Bus system eigenvalues shows that PSS and STATCOM add more damping to the system.
- Connection of a fixed-speed wind farm to an IEEE-14 Bus system via HVDC link shows an improvement in oscillatory modes and adds damping to the system.
- Time-domain simulation of a fixed-speed wind farm connected to an IEEE-14 Bus system via HVAC link shows oscillation instability, and the system takes a long time to recover from the applied three phase fault.
- PMSG reacts like STATCOM for voltage recovery by virtue of the full-scale back-to-back converter built inside PMSG wind generators.
- The HVDC link prevented the fault from reaching the wind farm by blocking it.

## ACKNOWLEDGMENT

The authors sincerely thank Saudi Arabia's Ministry of Higher Education for granting a scholarship.

## REFERENCES

- [1] K. R. Steve Sawyer, "Global Wind Report," belgium 2010.
- [2] K. R. Steve Sawyer, "Global Wind energy Outlook 2010," belgium 2010.
- [3] S. Heier, Grid Integration of Wind Energy Conversion System, 1998.
- [4] D. Thakur and N. Mithulananthan, "Influence of Constant Speed Wind Turbine Generator on Power System Oscillation," Electric Power Components and Systems, vol. 37, pp. 478-494, 2009.
- [5] G. Rogers, power system Oscillations: Kluwer Academic Publishers, 2000.
- [6] P. W. Sauer, Power System Dynamics and Stability: Prentice-Hall, Inc., 1998.
- [7] P. Kundur, Power System Stability and Control. New York: McGraw-Hill, Inc., 1994.
- [8] O. A. Almasari, "Low Frequency Oscillatory Stability Study of Power System with Wind Farms," Master Degree, School of Information Technology and Electrical Engineering, The University of Queensland, Brisbane, 2011.
- [9] W. Chen, S. Libao, W. Liming, and N. Yixin, "Small signal stability analysis considering grid-connected wind farms of DFIG type," in Power and Energy Society General Meeting - Conversion and Delivery of Electrical Energy in the 21st Century, 2008 IEEE, 2008, pp. 1-6.
- [10] A. F. Snyder, "Inter-Area Oscillation Damping with Power System Stabilizers and synchronized Phasor Measurements," Master thesis, Electrical Engineering, Virginia Polytechnic Institute and State University, 1997.
- [11] F. J. Swift and H. F. Wang, "The connection between modal analysis and electric torque analysis in studying the oscillation stability of multi-machine power systems," International Journal of Electrical Power & Energy Systems, vol. 19, pp. 321-330, Jun 1997.
- [12] J. G. Sloopweg and W. L. Kling, "The impact of large scale wind power generation on power system oscillations," Electric Power Systems Research, vol. 67, pp. 9-20, Oct 2003.
- [13] R. C. Burchett and G. T. Heydt, "Probabilistic Methods For Power System Dynamic Stability Studies," Power Apparatus and Systems, IEEE Transactions on, vol. PAS-97, pp. 695-702, 1978.
- [14] R. D. Fernández, R. J. Mantz, and P. E. Battaioito, "Impact of wind farms on a power system. An eigenvalue analysis approach," Renewable Energy, vol. 32, pp. 1676-1688, 2007.
- [15] D. Gautam, V. Vittal, and T. Harbour, "Impact of increased penetration of DFIG based wind turbine generators on transient and small signal stability of power systems," in Power and Energy Society General Meeting, 2010 IEEE, 2010, pp. 1-1.
- [16] Y. Sun, L. Wang, G. Li, and J. Lin, "A review on analysis and control of small signal stability of power systems with large scale integration of wind power," in Power System Technology (POWERCON), 2010 International Conference on, 2010, pp. 1-6.
- [17] D. Devaraj and R. Jeevajyothi, "Impact of wind turbine systems on power system voltage stability," in Computer, Communication and Electrical Technology (ICCCET), 2011 International Conference on, 2011, pp. 411-416.
- [18] G. Michalke and A. D. Hansen, "Modelling and control of variable speed wind turbines for power system studies," Wind Energy, vol. 13, pp. 307-322, May 2010.
- [19] I. D. Margaritis and N. D. Hatziargyriou, "Direct drive synchronous generator wind turbine models for power system studies," in Power Generation, Transmission, Distribution and Energy Conversion (MedPower 2010), 7th Mediterranean Conference and Exhibition on, 2010, pp. 1-7.
- [20] Kods S. K. M, Canizares C. "Modeling and Simulation of IEEE 14 Bus System with FACTS controllers", Technical report 2003-3, University of Waterloo, On, Canada, 2003.